

## High-performance type-II BiOI/CdS heterojunction photodetector for ultraviolet imaging and optical communication

Haoyue Wei<sup>1</sup>, Qihong Tan<sup>1,2,†</sup>, Ran Ma<sup>1</sup>, Peizhi Yang<sup>3</sup>, Yingkai Liu<sup>1,2</sup>, Qianjin Wang<sup>1,2,‡</sup>

<sup>1</sup>College of Physics and Electronic Information, Yunnan Normal University, Kunming 650500, China

<sup>2</sup>Yunnan Provincial Key Laboratory for Photoelectric Information Technology, Yunnan Normal University, Kunming 650500, China

<sup>3</sup>Key Laboratory of Advanced Technique & Preparation for Renewable Energy Materials, Ministry of Education, Yunnan Normal University, Kunming 650500, China

Corresponding authors. E-mail: <sup>†</sup>tanqihong1@126.com, <sup>‡</sup>[qjwang@xtu.edu.cn](mailto:qjwang@xtu.edu.cn)

Received December 30, 2025; accepted March 13, 2026

### Supporting Information

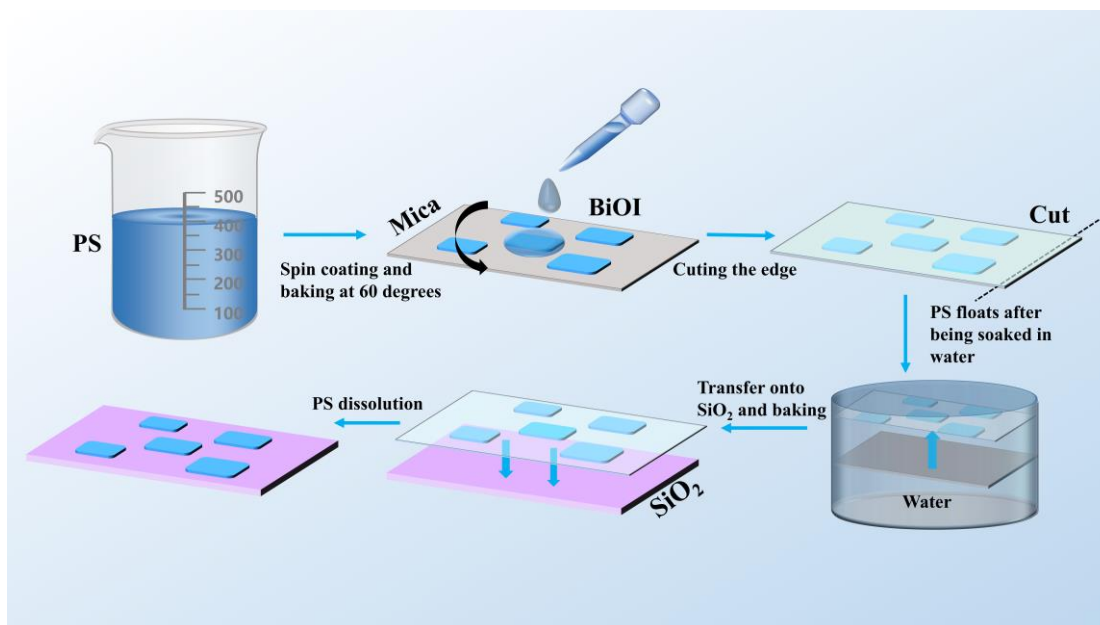


**Fig S1.** Schematic diagram of transferring BiOI nanosheets using a PS film.

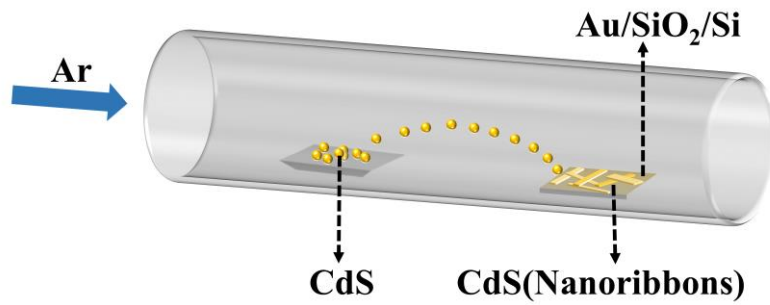


**Fig S2.** Schematic diagram of the growth process of CdS nanobelts.

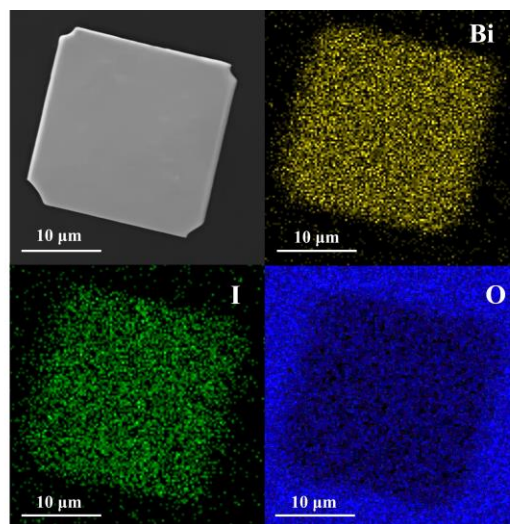


**Fig S3.** Scanning electron microscopy and EDS elemental composition of a single BiOI nanosheet.

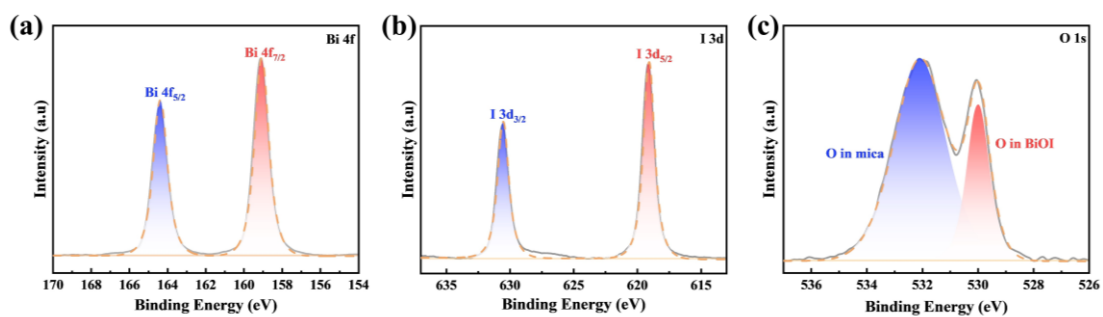


**Fig S4.** XPS spectra of BiOI nanosheets grown on mica. (a) Bi 4f, (b) I 3d, and (c) O 1s.

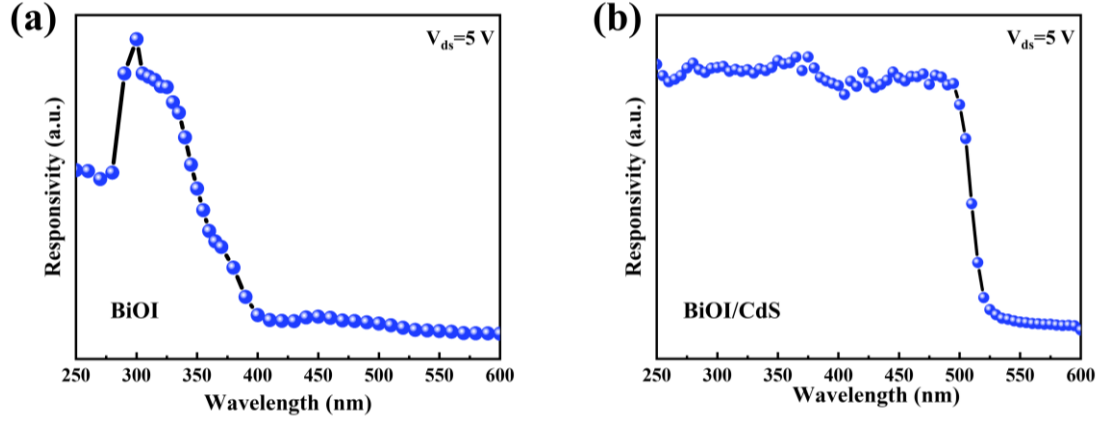


**Fig S5.** Spectral responsivity of (a) the 2D BiOI photodetector and (b) the BiOI/CdS heterojunction photodetector.

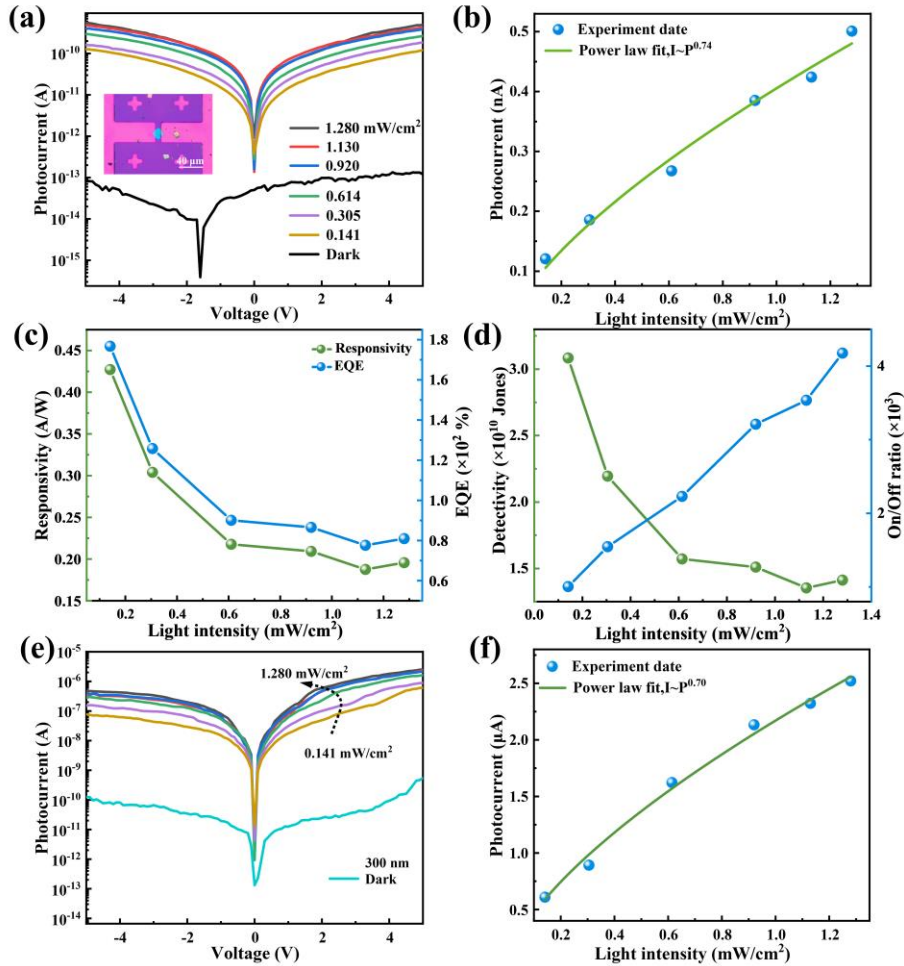


**Fig S6.** (a) Logarithmic  $I-V$  characteristics of the 2D BiOI photodetector in the dark and under 300 nm illumination at different optical power densities. (b) Fitting curve between optical power density and photocurrent at  $V_{ds} = 5 \text{ V}$ . (c) Corresponding  $R$  and  $EQE$ , (d)  $D^*$  and on/off ratio under different optical power densities. (e) Logarithmic  $I-V$  curves of the CdS nanobelt photodetector under the same conditions. (f) Corresponding power-law fitting results.

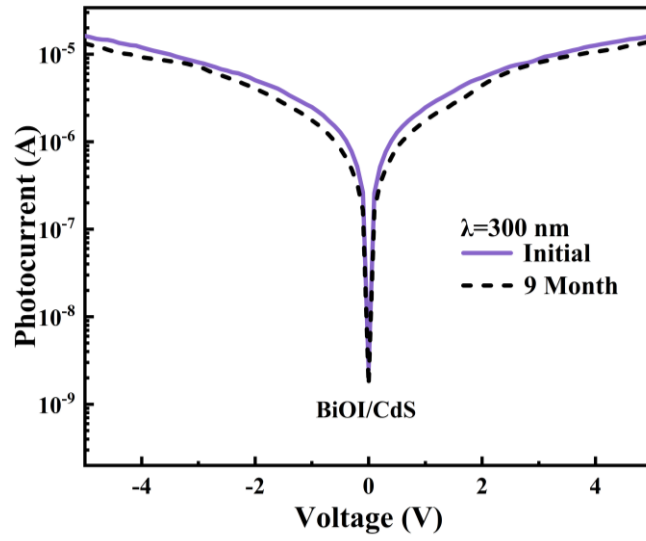


**Fig S7.** Photocurrent of BiOI/CdS device after 9 months of air exposure, measured under 300 nm illumination.

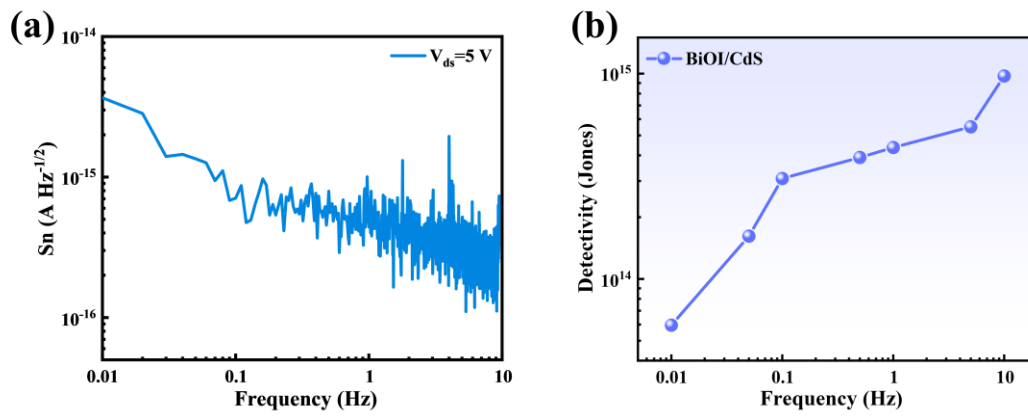


**Fig S8.** (a) Noise spectral density and (b) frequency-dependent  $D^*$  of the BiOI/CdS photodetector.

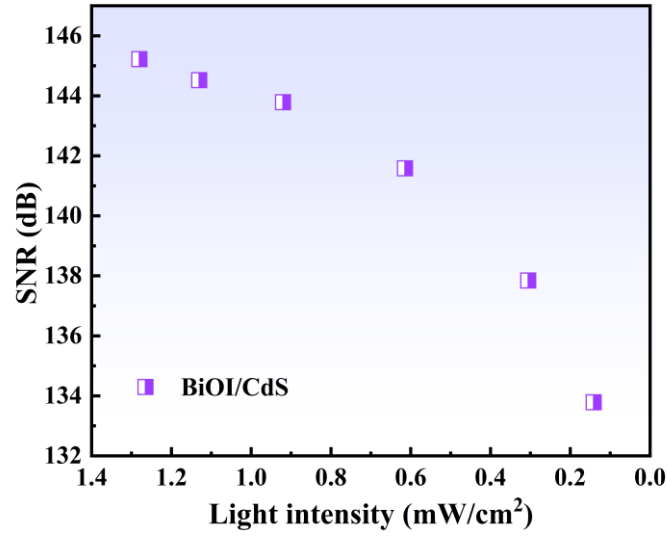


Fig S9. SNR measured at various optical power densities.

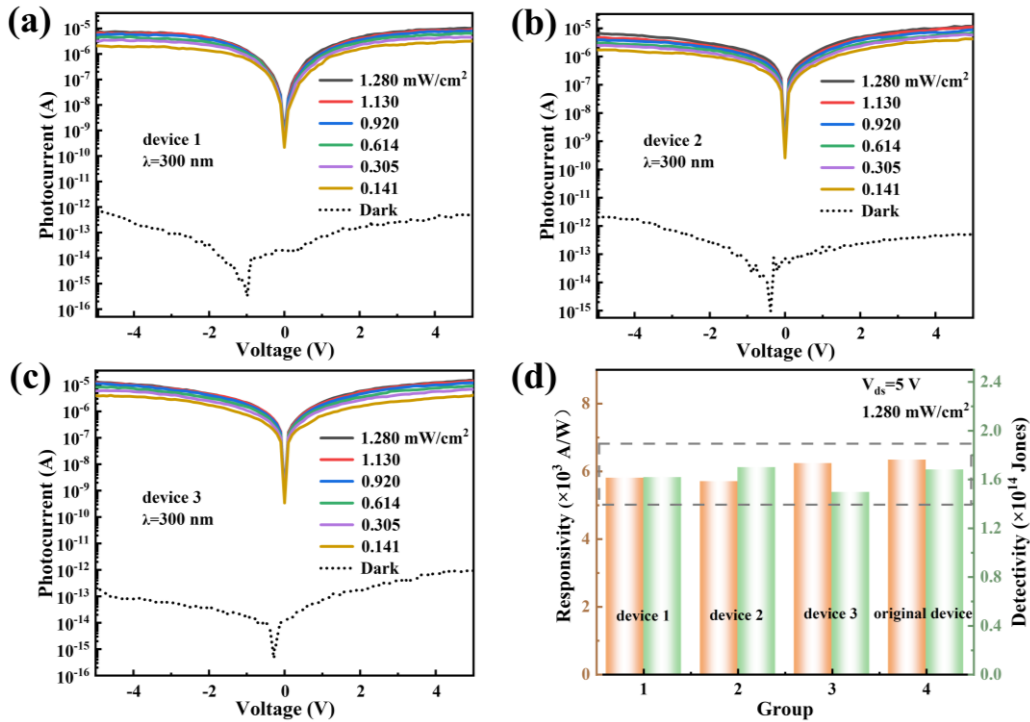


Fig S10. (a-c) The  $I$ - $V$  curves of three distinct devices under 300 nm illumination at different optical power densities are presented. (d) The  $R$  and  $D^*$  of the three devices under 300 nm illumination at a power density of 1.280 mW/cm<sup>2</sup>. The original device corresponds to the device reported in the main text.

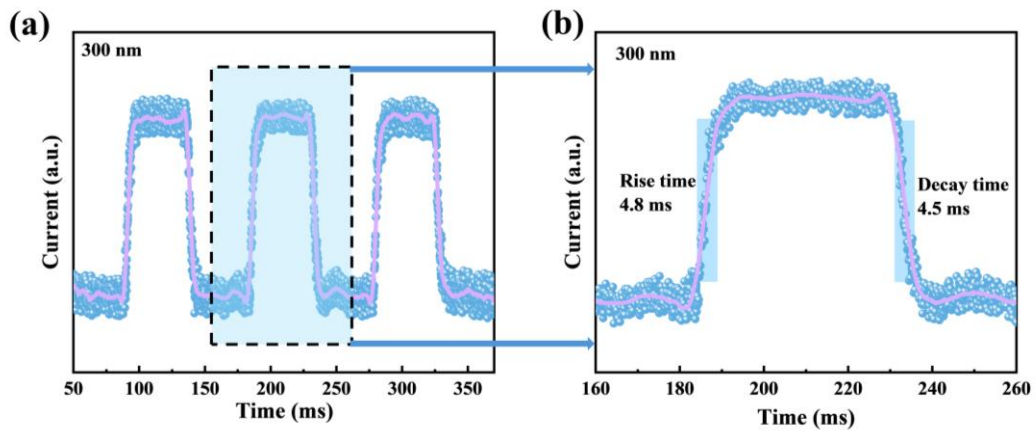


Fig S11. Rise and fall time of the 2D BiOI photodetector.

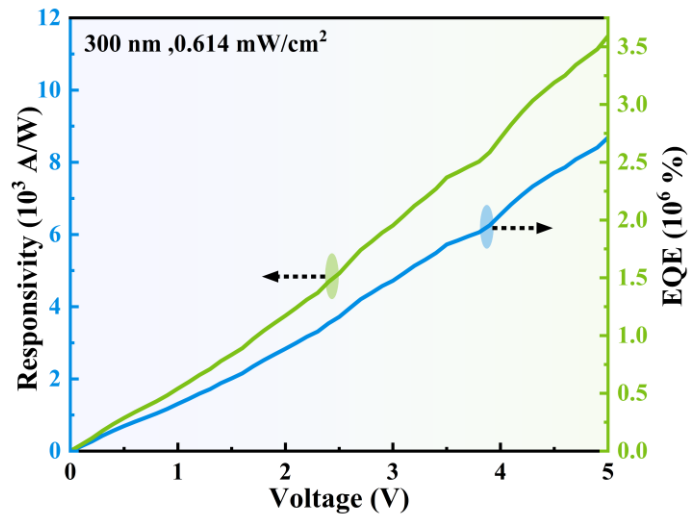


Fig S12. Dependence of  $R$  and  $EQE$  on the applied bias voltage at an incident power density of  $0.614 \text{ mW/cm}^2$  under 300 nm UV illumination.